The genome regulatory landscape of Atlantic salmon liver through smoltification

Thomas N. Harvey[1†], Gareth B. Gillard[1†], Line L. Røsæg[1†], Fabian Grammes[2], Øystein Monsen[3], Jon Olav Vik[4], Torgeir R. Hvidsten[4], Simen R. Sandve[1]*

Affiliations:

[1]*Centre for Integrative Genetics (CIGENE), Department of Animal and Aquacultural Sciences, Faculty of Biosciences, Norwegian University of Life Sciences, NO-1432 Ås, Norway*

[2]*AquaGen AS. P.O. Box 1240, NO-7462 Trondheim, Norway*

[3]*Michael Sars Centre, University of Bergen, 5008 Bergen, Norway*

[4]*Faculty of Chemistry, Biotechnology and Food Sciences, Norwegian University of Life Sciences, NO-1432 Ås, Norway*

† *contributed equally*

* *corresponding author*

Short title: Smolt genome regulation

Abstract

The anadromous Atlantic salmon undergo a preparatory physiological transformation before seawater entry, referred to as smoltification. Key molecular developmental processes involved in this life stage transition, such as remodeling of gill functions, are known to be synchronized and modulated by environmental cues like photoperiod. However, little is known about the photoperiod influence and genome regulatory processes driving other canonical aspects of smoltification such as the large-scale changes in lipid metabolism and energy homeostasis in the developing smolt liver.

Here we generate transcriptome, DNA methylation, and chromatin accessibility data from salmon livers across smoltification under different photoperiod regimes. We find a systematic reduction of expression levels of genes with a metabolic function, such as lipid metabolism, and increased expression of energy related genes such as oxidative phosphorylation, during smolt development in freshwater. However, in contrast to similar studies of the gill, smolt liver gene expression prior to seawater transfer was not impacted by photoperiodic history. Integrated analyses of gene expression and transcription factor (TF) binding signatures highlight likely important TF dynamics underlying smolt gene regulatory changes. We infer that ZNF682, KLFs, and NFY TFs are important in driving a liver metabolic shift from synthesis to break down of organic compounds in freshwater. Moreover, the increased expression of ribosomal associated genes after smolts were transferred to seawater was associated with increased occupancy of NFIX and JUN/FOS TFs proximal to transcription start sites, which could be the molecular consequence of rising levels of circulating growth hormones after seawater transition. We also identified differential methylation patterns across the genome, but associated genes were not functionally enriched or correlated to observed gene expression changes across smolt development. This contrasts with changes in TF binding which were highly correlated to gene expression, underscoring the relative importance of chromatin accessibility and transcription factor regulation in smoltification.

Author summary

45 Atlantic salmon migrate between freshwater and seawater as they mature and grow. To survive the

46 transition between these distinct environments, salmon transform their behavior, morphology, and

47 physiology through the process of smoltification. One important adaptation to life at sea is remodeling

48 of metabolism in the liver. It is unknown, however, whether this is a preadaptation that occurs before

49 migration, what degree this is influenced by day length like other aspects of smoltification, and how

50 gene regulatory programs shift to accomplish this transformation. We addressed these questions through

51 a time course experiment where salmon were exposed to short and long day lengths, smoltified, and

52 transferred to seawater. We sampled the livers and measured changes in gene expression, DNA

53 methylation, chromatin accessibility, and transcription factor binding. We found metabolic remodeling

54 occurred in freshwater before exposure to seawater and that day length did not have any long-term

55 effects in liver. Transcription factor binding dynamics were closely linked to gene expression changes,

56 and we describe transcription factors with key roles in smoltification. In stark contrast, we found no

57 links between gene expression changes and DNA methylation patterns. This work deepens our

58 understanding of the regulatory gear shifts associated with metabolic remodeling during smoltification.

Introduction

60 Atlantic salmon are an anadromous species. They begin life in freshwater riverine habitats, then migrate

61 to sea to grow and mature before returning to freshwater to spawn. The seawater migration is preceded

62 by a "preparatory" process that influences a range of behavioral, morphological and physiological traits,

63 referred to as smoltification [1]. This includes changes in pigmentation and growth [2], ion regulation

64 [3, 4], the immune system [5], and various functions of the metabolism [6, 7].

65 The timing of smoltification is regulated by the physiological status of the fish [8], as well as external

66 environmental signals such as temperature and day length [2, 9, 10]. Salmon smoltify in the spring, and

67 the transition from short to long days is believed to drive changes in hormonal regulation and initiate

68 smoltification. In line with this model, we recently demonstrated that exposure to a short photoperiod

69   (i.e. a simulated winter photoperiod) induce transcription of a subset of photoperiod-history sensitive

70   genes [3], dampens acute transcriptomic responses to increased salinity, and results in enhanced

71   seawater growth [11]. These findings support a model of smolt development regulation, where

72   photoperiodic-history drives genome regulatory remodeling underlying key smoltification associated

73   phenotypes.

74   Although gill physiology has received most attention in the smoltification literature, other organs such

75   as the liver also undergo large changes in function upon smoltification and seawater migration, with

76   large implications for key metabolic traits. It has been shown that lipid composition in Atlantic salmon

77   reared on different diets converges after smoltification [12, 13]. This is likely a consequence of

78   smoltification associated increase in lipolytic rates and decreased lipid biosynthesis [6, 7]. In a recent

79   study we demonstrated large changes in lipid metabolism gene regulation across the fresh-saltwater

80   transition following smoltification [14]. Unfortunately, in this study smoltification and seawater transfer

81   were confounded (i.e. smolts in freshwater were not sampled), hence it remains unclear if photoperiodic

82   history is involved in shaping the molecular phenotype of the smolt liver as we observe in gills.

83   In this study, we conducted a smoltification trial to test if the photoperiodic history is a major factor

84   impacting the genome regulatory landscape of Atlantic salmon liver. To do this we generated

85   transcriptome, chromatin accessibility, and DNA methylation data across the smolt development and

86   seawater transfer to characterize the transcriptomic changes in smolts reared with a short winter-like

87   photoperiod (8:16) compared to smolts reared on constant light (24:0). We test if photoperiodic history

88   affects the smolt liver phenotype at the level of gene expression and use chromatin accessibility data to

89   identify putative regulatory pathways and transcription factors involved in life-stage associated changes

90   in liver function from the juvenile stage in the freshwater environment to an adult fish in seawater.

Results

Gene expression changes support decreased lipid metabolism and increased protein metabolism and energy production during smoltification

A main goal was determining the effects of smoltification on metabolism and whether there was an effect of exposure to a short photoperiod (i.e. a winter) on the gene regulation in the liver. To accomplish this, we reared three groups of salmon for 46 weeks on commercial diets, from parr, through smoltification, and 6 weeks following transfer to seawater (Fig 1). The experimental group was given an artificial winter-like short photoperiod (8 hours light, 16 hours dark) for 8 weeks before they were returned to constant light, while the control group was reared under constant light throughout the experiment. Finally, the freshwater control group contained fish from the experimental group that was not transferred to sea. Following smoltification, fish transferred to seawater grew more slowly than fish that remained in freshwater (Fig 1, Table S1). There was no mortality throughout the freshwater portion of the trial, but some mortality (8x fish) in one tank due to improper oxygenation after seawater transfer.


Fig 1: Salmon growth over time. Schematic of the experimental design and weight of salmon over time. Fish were reared for 21 weeks after first feeding in constant light conditions prior to week 1 sampling. The experimental group (black, solid line) was exposed to a short photoperiod before switched back to constant light and sampled at week 10. After a smoltification period, fish were sampled at week 19, then transferred to seawater conditions and sampled lastly at week 25. A photoperiod control group (grey, dashed line) received constant light throughout the experiment, and a freshwater control

111   group branched off from the experimental group by remaining in freshwater. Four fish were sampled at

112   each timepoint.

113

114   To characterize global transcriptome changes through key life stages, under a semi-natural

115   developmental trajectory, we sampled liver tissue from fish at each sampling point for RNA sequencing.

116   We first tested for changes in gene expression in fish experiencing artificial winter and transfer to

117   seawater (experimental group) using an ANOVA-like test. This yielded 3,845 differentially expressed

118   genes (DEGs, FDR <0.05) which were assigned to seven co-expression clusters using hierarchical

119   clustering (Fig 2A, Table S2). These clusters reflected major patterns of gene regulatory changes (Fig

120   2B); peak expression levels in smolts (clusters 2 and 3), peak expression following the short photoperiod

121   (clusters 4 and 5), decreased expression after short photoperiod and in smolts relative to all other time

122   points (cluster 6), steady decrease in expression from parr throughout the experiment (cluster 7), and

123   strong increase in expression in seawater (cluster 1).

124   To associate well defined metabolic or signaling processes to the different gene expression trends, we

125   performed KEGG enrichment analysis on each co-expression cluster, yielding 56 unique significantly

126   enriched (adjusted p <0.05) pathways (Fig 2C). Genes in clusters 2 and 3 that increased during

127   smoltification and sharply decreased after seawater transfer were enriched in pathways related to

128   genetic information processing, cell growth, protein metabolism, and oxidative phosphorylation. Genes

129   in clusters 4 and 5 which had peak expression after a short photoperiod and decreased during

130   smoltification and seawater transfer were similarly enriched in genetic information processing pathways

131   and energy metabolism, however they also contained several pathways related to amino acid

132   metabolism including cysteine and methionine metabolism, glutathione metabolism, and

133   selenocompound metabolism. Cluster 1 genes strongly increased in relative expression after seawater

134   transfer and was exclusively enriched in the ribosome pathway. Genes in cluster 7 which decreased in

135   relative expression during smoltification and remained low during seawater transfer were enriched

136   mainly in lipid, amino acid, and carbohydrate metabolic pathways, ABC transporters, and signaling

137   pathways including FoxO signaling and PPAR signaling.

6
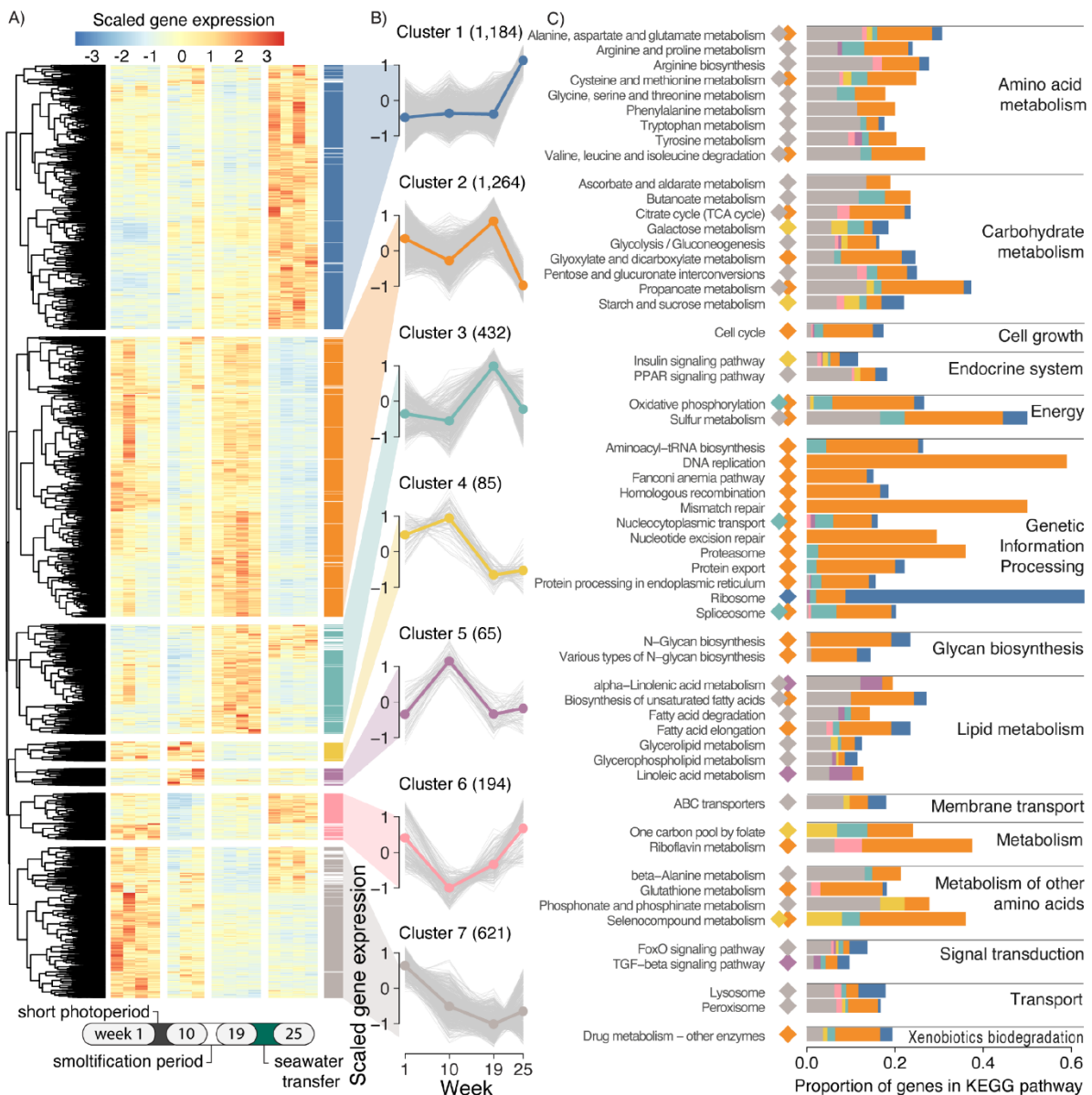
Fig 2: Global gene expression changes across life-stage. A) Relative liver expression of genes differentially expressed between any time point in the experimental fish cohort (FDR <0.05). Scaled expression is denoted as gene-scaled transcripts per million. Genes were partitioned into six co-expression clusters by hierarchical clustering. Colored bars indicate cluster membership when correlation to the mean cluster pattern was >0.5. Genes with correlation =<0.5 were excluded. B) Gene expression trends over time by cluster. Colored line indicates mean relative expression while grey lines are individual genes within the cluster. C) KEGG pathway enrichment by cluster. Colored diamonds indicate for pathways which clusters they are significantly enriched in (adjusted p <0.05). Colored bars indicate the proportion of genes within the pathways that are in clusters.

7

148   Since many KEGG pathways contain enzymes with reciprocal activities, we manually examined genes

149   within select enriched KEGG pathways to determine what was driving enrichment trends. In lipid

150   metabolic pathways we observed a distinct bias in genes relating to long-chain fatty acids towards

151   downregulation in freshwater smolts. Seven long-chain-fatty-acyl-CoA ligase (*acsl*) genes (*acsl1*, three

152   *acsl3* and three *acsl4*), acetyl-CoA carboxylase (*acc1*), three acetyl-CoA synthetase genes (*acs2l-1*,

153   *acs2l-1*, and *acs2l-1*), several key genes related to polyunsaturated fatty acid (PUFA) biosynthesis (*5fad*,

154   *6fada*, *6fadb*, *elovl5b*, and *elovl2*), both copies of fatty acid synthase (*fas1* and *fas2*), and three copies

155   of the key gene diacylglycerol acetyltransferase (two *dgat1* and one *dgat2*) all significantly decreased

156   during smoltification and remain lowly expressed through seawater transfer (Fig 3B).
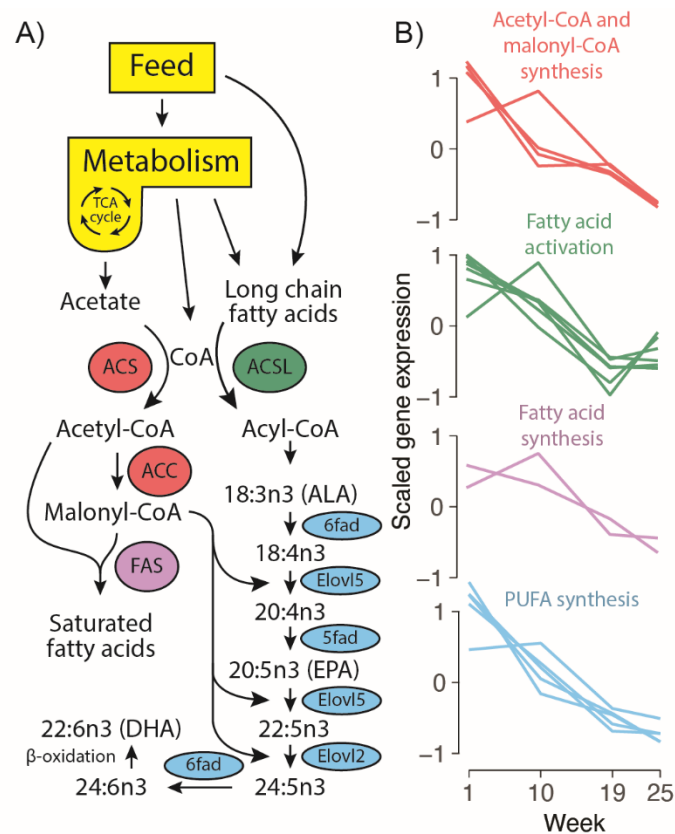
157

158   **Fig 3: Expression of key lipid metabolism genes across the parr-smolt transition.** A) Schematic of

159   the lipid biosynthesis pathway in Atlantic salmon. B) Relative expression of genes in the pathway over

160   time. Acetyl-CoA and malonyl-CoA synthesis (red) displays genes *acc1*, *acs2l-1*, *acs2l-2*, and *acs2l-3*.

161   Fatty acid activation (green) displays genes *acsl1*, *acsl3l-1*, *acsl3l-2*, *acsl3l-3*, *acsl4*, *acsl4l-1*, *acsl4l-2*.

8

162   Fatty acid synthesis (purple) displays gene *fas1* and *fas2*. Poly unsaturated fatty acid (PUFA) synthesis

163   (blue) displays genes *5fad*, *6fada*, *6fadb*, *elovl2*, and *elovl5b*.

164

165   Synthesis of acetyl-CoA by *acs* and activation of long-chain fatty acids by *acsl* is the first obligatory

166   step for entry into beta-oxidation or biosynthesis pathways (Fig 3A), so a decrease in these gene

167   products likely means that metabolism of their substrates (acetate and C12 to C20 fatty acids) also

168   decreases [15]. Finally, three copies of the key gene diacylglycerol acetyltransferase (two *dgat1* and

169   one *dgat2*) which catalyzes the last committed step in triacylglycerol biosynthesis [16] decreased in

170   freshwater smolts. Collectively, co-downregulation of these important lipid associated genes is a strong

171   indicator of decreased utilization and processing of fatty acids, especially long chain poly unsaturated

172   fatty acids (LC-PUFA), in smolts preparing to enter a seawater environment.

173   We identified genes directly influenced by seawater transfer by performing a pair-wise test for gene

174   expression changes between the experimental group and freshwater control group at week 25. This

175   resulted in 2,121 DEGs (FDR <0.05, Table S5), most (1227) being downregulated in seawater compared

176   to freshwater (Fig S1) and overlapped with many genes belonging to co-expression clusters 1 (281) and

177   cluster 2 (529) in Fig 2. Regarding lipid metabolism, processes related to de novo fatty acid synthesis

178   decrease in seawater relative to control. Both copies of fatty acid synthase (*fas1* and *fas2*) and one

179   acetyl-CoA carboxylase (*acc1*) decreased expression in seawater, all of which catalyze key steps in *de*

180   *novo* fatty acid synthesis [17]. Additionally, two other *acsl* genes (*acsbg2* and *acsl1*) known to be

181   involved in saturated and monounsaturated fatty acid activation were downregulated in seawater [18].

182   This coincided with an increase in several thioesterase genes, including *acot1l* and *acot5l*, responsible

183   for de-activation of fatty acids through the hydrolysis of acyl-CoAs [19]. It is unlikely that de-

184   smoltification occurred in the freshwater control smolts because expression of these genes remains

185   stable between weeks 19 and 25 in the control fish. This combination of decreased expression of key

186   *de novo* biosynthesis genes and increased fatty acid de-activation through greatly increased thioesterase

187   expression suggests a reduced capacity to synthesize fatty acids in liver of fish after transition to sea, in

188   line with previous findings [14].

9

No long-term effect of short photoperiod exposure in liver

189

190 To evaluate the role of photoperiodic history on the development of liver function during smoltification,

191 we performed pair-wise tests for gene expression changes between experimental fish exposed to a short

192 photoperiod and control fish on constant light regime at week 10 (at the end of the short photoperiod

193 exposure) and at week 19 (just prior to seawater transfer). We identified a relatively shorter list of DEGs

194 (532, FDR <0.05, Table S3) associated with photoperiodic history differences at week 10, but only a

195 few DEGs at week 19 (15, Fig 4, Table S4). At week 10 we found a vitamin D 25-hydroxylase gene,

196 the first step in the formation of biologically active vitamin D [20], was strongly downregulated after a

197 short photoperiod. This is likely due to decreased UV mediated vitamin D synthesis in the skin from

198 less exposure to light [21]. The low number of DEGs at week 19, and low overlap between week 10

199 and 19 expression changes, showed that different photoperiodic histories did not impact longer term

200 gene function in the liver following smoltification.
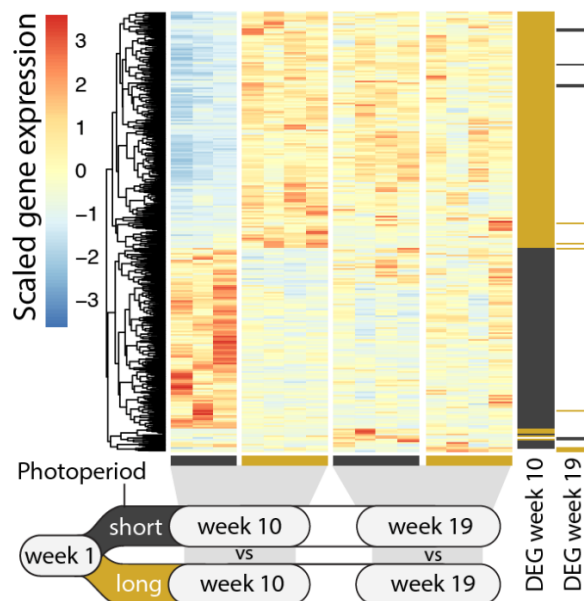
201

202 **Fig 4: Gene expression changes in response to photoperiod history.** Relative liver expression of

203 differentially expressed genes (DEGs, FDR <0.05) between the short photoperiod exposed experimental

204 group and long photoperiod control group at weeks 10 and 19. Genes are marked to the right if

205 differentially expressed higher (black) or lower (yellow) in response to a short photoperiod at weeks 10

206 and/or 19.

10

207

Remodeling of liver transcription factor binding across smoltification

209 To better understand the mechanistic drivers shaping changes in liver gene expression through salmon

210 life stages, we generated ATAC-seq data to measure accessibility of chromatin and used this to indirectly

211 quantify transcription factor (TF) occupancy at predicted TF binding sites (TFBS) by assessing local

212 drops in chromatin accessibility (aka footprints). For each time point across the 25 week experiment

213 group we generated two replicate samples of ATAC-seq data from the same livers sampled for RNA-

214 seq, at a depth of 55-72M reads. Reads were aligned to the genome (41-63M) and peaks where reads

215 were concentrated were called to represent regions of accessible chromatin. A unified set of the ATAC

216 peaks was made by merging peaks across the different weeks (File S1). A principal component analysis

217 (PCA) on the sample's read counts over the unified peaks showed pairing of replicates and separation

218 between the weeks (Fig 5A). PC1 separated weeks 1 and 19 to 10 and 25, while PC2 separated the pre-

219 smolt weeks (1 and 10) to the post-smolt (19 and 25). The unified set of 201k peaks was composed of

220 peak sets from each week, with week 19 having the highest number of peaks (181k, Fig 5B). Most of

221 the peaks at each week were shared across sets, with week 19 standing out as having the greatest number

222 of unique peaks (Fig 5C). Peaks were highly concentrated around the TSS of genes as expected,

223 associating with gene regulation (Fig 5D). Peaks were mostly found in introns or intergenic regions,

224 suggesting a higher proportion of peaks at enhancer than promoter elements, not unexpected (Fig 5E).
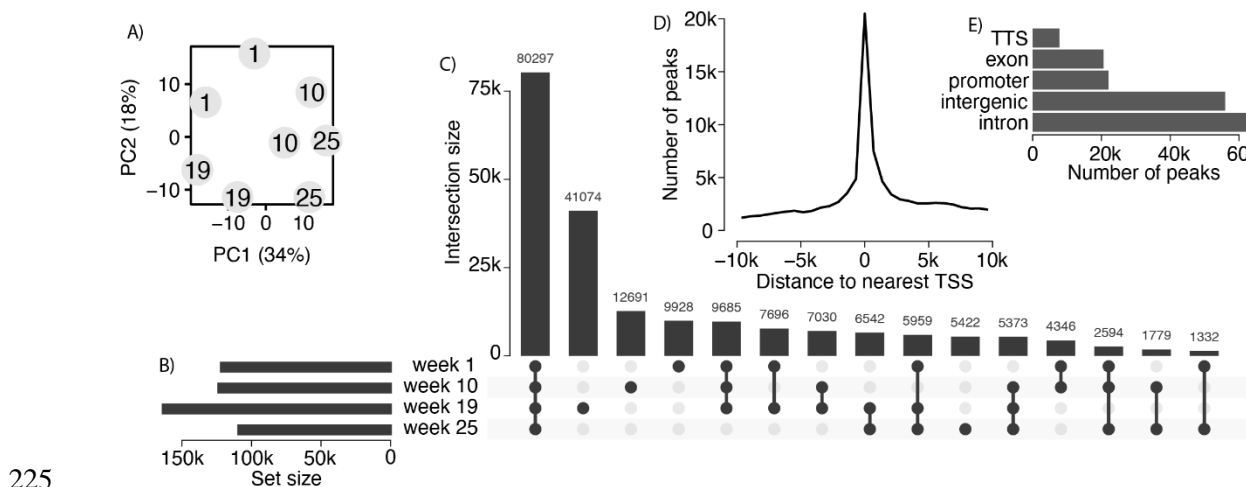

225

226 **Fig 5: Comparison of chromatin accessibility across life-stage.** A) Similarity of ATAC-seq samples

227 at different weeks by principal component (PC) analysis of ATAC-seq read counts within a unified set

228 of ATAC peaks (shared and unique between weeks). B) Number of ATAC peaks called at each week.

229 C) Number of peaks intersecting between sets or unique to each week. D) Distribution of distances (in

230 base pairs) of unified peaks to the nearest gene transcription start site (TSS). E) Genomic locations of

231 unified peaks.

232

233 Little is known about the environmentally driven changes in gene regulatory pathways in salmon. We

234 therefore used a TF footprinting analysis to identify within peaks drops in reads at TFBS, indicating a

235 bound TF (i.e. occupancy) at that site in the given sample. We first describe the TFs showing genome-

236 wide changes in TFBS binding between livers sampled in different photoperiods and water salinities

237 (Table S6). Since developmental stage (age) can also impact TF binding patterns, we focused on TFs

238 with differences in occupancy that persists across environmental contrasts with fish from different

239 developmental stages (Fig 6A and B). Using a cutoff for differential TF occupancy ($\log_2$ fold change in

240 genome wide TF-motif occupancy >0.1) we identified 33 and 35 TF binding motifs that were associated

241 with photoperiod and salinity, respectively (Fig 6C, Table S7).

242 Most (30/35) TF motifs associated with water salinity differences were found to have a marked drop in

243 genomic occupancy after transition to saltwater (Fig 6C). These include several motifs known to bind

244 TFs associated in energy homeostasis related processes, such as TEF's, GATA4, NR5A1 MAF, KLFs

245 [22-24]. Only five TF motifs had a significantly higher occupancy in saltwater, including LIM's and

246 two homeobox binding motifs (PHOX2B and HOXC8). The photoperiod contrast (Fig 6B and 6C)

247 revealed that most TFBS's with induced occupancy after a short day period were binding sites for E-26

248 family transcription factors (ETS, ERG, ETV, SPIC, ELK, SPI1), which have been associated with

249 regulation of circadian genes in other species [25, 26]. It is interesting to note that these TF binding

250 sites with a spike in occupancy after a short photoperiod drops dramatically towards the end of

251 smoltification (week 19) and stays low after seawater transfer (week 25). TF binding sites with reduced

252 occupancy following a period of shorter days were mostly related to homeostasis of cellular

12

253 metabolism, including key liver glucose and lipid metabolism regulators PPARD [27], RXRs [28] and

254 HNF4A [29], as well as occupancy of thyroid hormone receptor beta (THRB) [30].

255
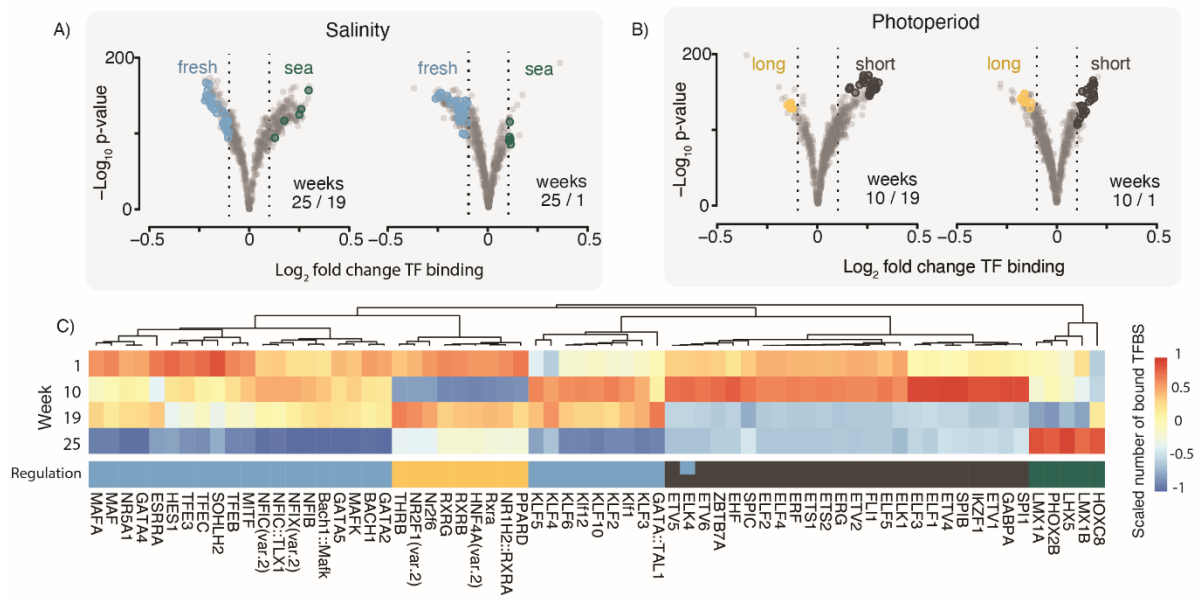
Fig 6: Genome wide changes in transcription factor activities across key life stages. Volcano plots

show genome wide fold changes and significance for transcription factor binding site (TFBS) binding

scores between A) fresh- to saltwater weeks and B) short to long photoperiod weeks. Transcription

factor (TF) motifs with significant changes in global binding scores (absolute $\log_2$ fold change >0.1)

across each contrast are colored. C) Heatmap shows the scaled number of total bound TFBS across the

weeks for the TF motifs that are significant in A) and B). The 'regulation' color indicates in which

environment the TF motif had the greater TFBS binding score.

263

264 Next, we wanted to link TF binding patterns to the specific gene regulatory dynamics. We assigned TF

265 motifs to genes (i.e. motif-gene pairs) by closest proximity and asked if genes with a particular

266 expression pattern (Fig 7A) were enriched for TF motifs in proximity with a corresponding pattern of

267 TF occupancy (Fig 7B). For example, for genes in expression cluster 1 with highest expression at week

268 25, we expect nearby binding sites to be enriched in TF motifs that are occupied by TFs in week 25, but

269 not the other time points. Indeed, genes in most expression clusters displayed significant enrichments

270 of TF motifs with expected binding patterns (colored red or orange), and these signatures were quite

13

271   distinct for each gene expression cluster (Fig 7C, Table S8). A diagram shows the comparison for the

272   fisher's exact tests between gene expression cluster and TF binding times to find TF motif significance

273   (Fig 7D).

274   From the enrichment results (Fig 7C) we see genes in cluster 1, enriched for ribosome related functions,

275   had nearby TFBS with NFIX binding following transition to seawater. This is a transcriptional regulator

276   known to be involved in ribosome biogenesis [31]. In addition, cluster 1 TFBS were associated with

277   binding of FOS and JUN after seawater entry. These TFs are major components of the Activator Protein

278   1 (AP-1) transcription factor complex which is responsive to growth factors and drive cell proliferation

279   and differentiation [32-34]. The top associated TFs for cluster 2 genes were ZNF341 known to be

280   involved in immune homeostasis [35] and several Fox TFs (A, F, L, I, K) linked to various cell

281   physiological processes [36, 37]. Cluster 3 genes were associated with several unnamed zinc finger

282   transcription factors (ZNFs and ZBTBs) binding at week 19 prior to seawater transfer, as well as binding

283   of RREB1 and EGR1 in week 19 and week 25. Among TFs with binding in week 19 only, we find genes

284   linked to regulation of immune cell function (ZBTB32 and ZNF263) [38, 39] as well as oxidative

285   phosphorylation [40]. The RREB1 and EGR1 are well described players in RAS signaling pathways

286   [41-43] involved in cell growth and proliferation. Among cluster 4 genes we find enrichment of insulin

287   and sugar metabolism functions, with PKNOX1 and NFYB TF binding significantly associated with

288   their expression patterns. Both these TFs have been shown to function in lipid metabolism and be linked

289   to insulin signaling [44-46]. The top TFs associated with cluster 6 gene expression is NR1D1 (also

290   called Reverbα), a core component of the circadian clock and regulator of lipid metabolism [47]. Cluster

291   6 is not enriched for any KEGG pathways but has a marked drop in expression after the short

292   photoperiod exposure. In the final cluster 7, enriched for genes playing roles in amino acid, glucose,

293   and lipid metabolism, we find very strong associations with binding of several TFs, including KLF and

294   SP family members. Indeed, these TFs are known to play important roles in regulating gluconeogenesis

295   and lipid and amino acid metabolism in mammalian livers [24, 48].

14
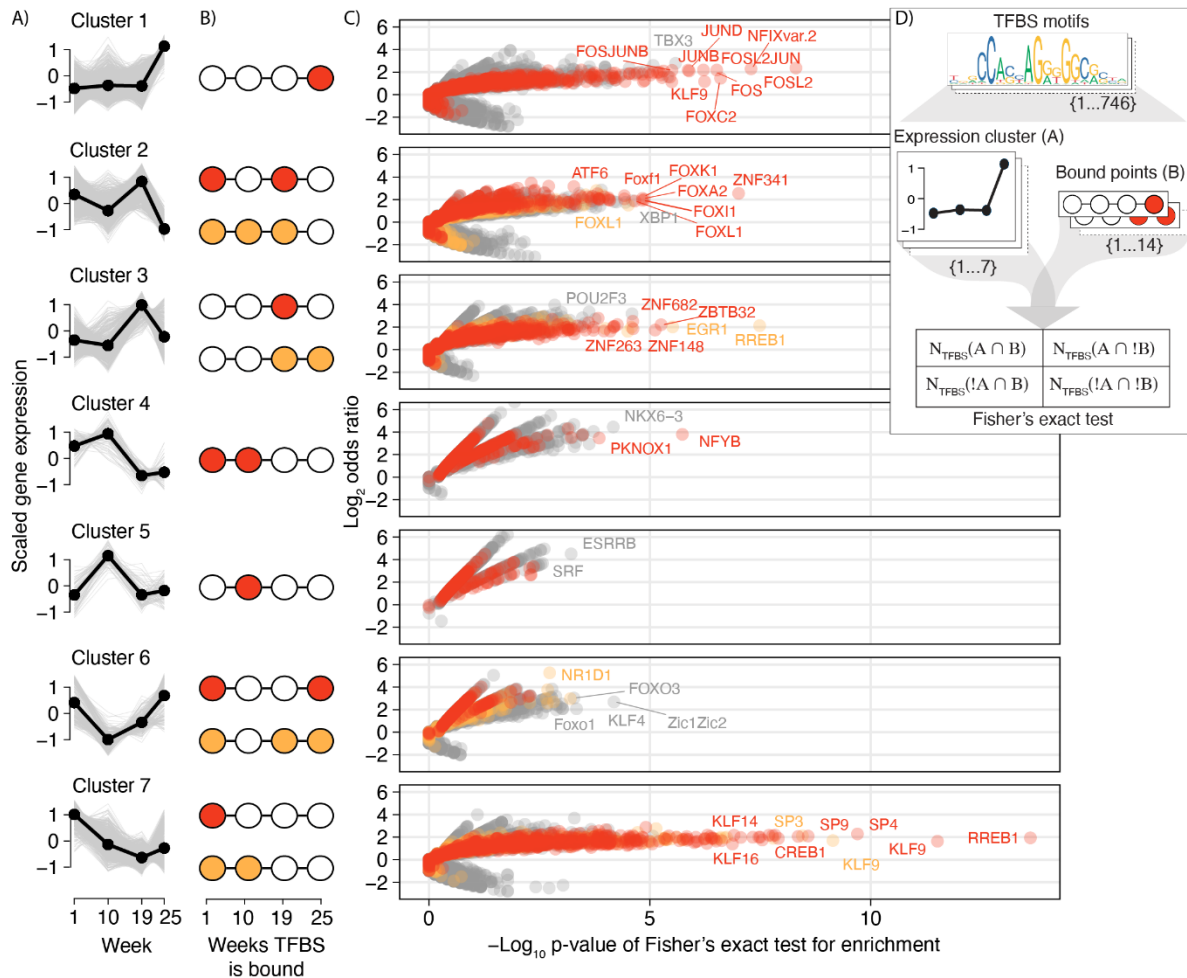
Fig 7. Enrichment of transcription factor binding patterns within gene expression clusters. A) Gene expression trends of clusters from Fig 1. B) Assumed weeks the transcription factor binding sites (TFBS) near genes in the cluster would be bound by a transcription factor (TF) to regulate transcription at the weeks of highest expression. A primary and secondary assumed binding pattern is colored red and orange respectively. C) For each set of genes in a cluster, each TF was tested if the TFBS near to those genes were enriched for any combination of binding pattern. Fisher's exact test results for all TF-binding pattern combinations are plotted per cluster as odds ratios against the significance. The test results for the assumed primary and secondary binding patterns in B) are colored red and orange, respectively. A top proportion of the most significant TFs (in a top quantile per test) are labeled. D) Diagram showing how each combination of TFBS motif, expression cluster, and binding pattern was tested for enrichment with a Fisher's exact test.

15

DNA methylation not linked with gene expression

To investigate the role DNA methylation had on the gene expression changes throughout salmon life-stages, we produced a RRBS dataset from the same liver samples at a depth of 26-40 M reads. A consensus set of 1.2M CpG positions was used for differential methylation analysis (Table S9). To assess genome wide differences in the regulation of CpG methylation, a principal component analysis (PCA) separated samples based on the methylation levels across the CpG consensus set. There was no clear separation of samples by timepoint or experiential condition, with PC1 and PC2 each explaining less than 5% of the variance (Fig S3A). To find specific sites of differential methylation, we tested all CpGs for differences in methylation score across any timepoints of the experimental group with an ANOVA-like approach (Table S10). Out of the consensus set of CpGs, 2535 (0.2%) were differentially methylated cytosines (DMC) across life-stages (FDR <0.05, fold change $>25\%$, Fig S3D-F). 209 of these were present in promoter regions, 103 in exons, 664 in introns, and 782 in intergenic regions (Fig S3E). Most genomic regions with a DMC had one differentially methylated site and only a few regions contained longer stretches (up to 26 bp in an intron) of differentially methylated CpGs (Fig 3D). We assessed if these CpGs were associated to genes with a specific function, but enrichment tests for GO or KEGG terms gave no significant results. We looked at next if the methylation percentages of DMCs correlated to changes in their corresponding gene's expression across timepoints. 157 DMC-gene pairs were significantly correlated (p <0.05, Pearson correlation coefficient >0.95), however most of these genes were relatively lowly expressed. Simulating random DMC-gene pair correlation values found that the distribution of values from our real data was not significantly different from that of simulated pairs (p-value <0.62, Fig S3G), refuting strong links between regulation of CpG methylation and gene expression in our experiment.

16

Discussion

Lipid metabolism remodeling as a pre-adaptation to life at sea

An important feature of smoltification is how the process prepares the juvenile fish for a life in sea, i.e. physiological necessities for survival are already present while the fish is still in freshwater. This is well documented for the osmoregulatory machinery in the gills [49-54]. For example, the likely causal agent for saltwater tolerance, NKA a1b, increases in abundance in freshwater gill tissues [8]. While lipid metabolism related gene expression is known to decrease in liver of seawater stage Atlantic salmon [14], this is the first report that systemic downregulation of lipid metabolism gene expression actually occurs before transition to sea (Figs 2 and 3). Given the availability of polyunsaturated fatty acids in seawater environments is higher than freshwater [55], and that the body lipid composition changes to match this in freshwater smolts [56], it is likely that the observed decrease in lipid metabolism is a genetically programmed preadaptation to life at sea. This study therefore adds another feature to the list of pre-adaptations in freshwater smolts.

The effect of photoperiod history on genome regulation during smolt liver development

Decades of research have revealed that many features of smolt physiology development can be affected by photoperiodic history [3, 57-64], including gene expression patterns. For example, a recent study of gill transcriptomes identified a subset of 96 genes with significantly increased gene expression levels in smolt exposed to a short photoperiod (8:16) during development compared to smolts kept on constant light (24:0) [3]. In this study, however, no long-term effects of short photoperiod exposure were found in liver transcriptomes (Fig 4). We do, however, show that salmon liver gene regulation is responsive to variation in photoperiods. Transcriptome profiles through smolt development show distinct gene sets with increased and decreased expression after reduction in photoperiod (Fig 2A clusters 5 and 6). Furthermore, analyses of TF binding dynamics (Fig 6) identify photoperiod sensitive TFs encoded by genes known to have repressed expression under short photoperiod in mammals, such as retinoic acid

17

356   related TFs (RXRs) and thyroid hormone receptors (THRB) [65, 66]. In addition, our integrated

357   analyses of gene expression profiles and TF binding (Fig 7) associated NR1D1, a core component of

358   the mammalian circadian clock [47], with genes having lower expression after exposure to short

359   photoperiod. Taken together, we conclude that smolt liver development does not seem to rely on having

360   experienced a winter-like photoperiod. Yet since acute effects of reduced photoperiods had a large

361   impact on gene regulatory networks related to metabolism (Figs 6 and 7), it is likely that highly

362   divergent photoperiodic histories can lead to delayed spillover effects and result in differences in

363   metabolic states.

Linking genome regulatory layers to understand the developing smolt liver

365   Salmon experience gene regulatory changes [13, 14] and function [6, 7] in liver during smolt

366   development in freshwater, and following seawater entry. Yet, no genome wide studies of DNA

367   methylation and TFs involved in driving these transcriptional and physiological changes have been

368   conducted. Here, we generated an RRBS dataset as well as an ATAC-seq dataset across smolt

369   development in liver and used the latter to predict TF occupancy dynamics and map out putative major

370   regulators of key developmental processes during smoltification (Figs 6 and 7).

371   Firstly, we showed that dynamic DNA methylation has a limited role in gene regulation in the liver

372   during smoltification. Of the 1.17 M CpGs in our dataset, only about 2500 of these showed dynamic

373   methylation during smoltification, and few of these were in the vicinity of differentially expressed

374   genes. This echoes an earlier study on methylation changes associated with early maturation in Atlantic

375   salmon in which the liver exhibits less dynamic methylation overall than brain and gonads [67]. Also

376   in other organs of Atlantic salmon, gene expression changes seem to be controlled by other gene

377   regulatory features than DNA methylation [68]. Despite the intriguing hypothesis of DNA methylation

378   being an important gene expression regulator, and an epigenetic one at that, our study questions this

379   role in the context of post-embryonic development. Indeed, many studies describe methylome changes

380   during metamorphosis or other post-embryonic transitions but does not provide strong evidence for a

381   causative connection between changes in gene expression and changes in DNA methylation [69-71].

Previous studies of liver physiology during parr-smolt transformation highlights decreased lipid and glycogen biosynthesis and increased levels of glyco- and lipolysis [7]. In line with this, about 600 genes enriched for lipid, carbohydrate, and amino acid metabolism related functions displayed a clear decreasing trend in gene expression from parr (week 1) to smolt (week 19) (Fig 2, cluster 7). Several TFs showed highly significant TFBS binding associations with the cluster 7 gene expression profile (Fig 7C) including KLF/SP gene family members known to play important roles in regulating gluconeogenesis and lipid and amino acid metabolism in mammalian livers [24, 48]. Finally, genes in expression cluster 4, also showing a marked decrease in expression in smolts (week 19), were enriched for TFBS that had a significant drop in NFY binding from week 19. This TF is known to be a major regulator of lipid metabolism, including biosynthesis of fatty acids [44]. Concurrently, but with opposite expression trends, genes involved in oxidative phosphorylation related functions (the last step in breaking down amino acids, lipids, and carbohydrates to energy) increased in expression from parr to smolts (Fig 2, cluster 3). The TFBS of these same genes were enriched for binding of the TF ZNF682 in smolts in week 19 (Fig 7C), a nuclear encoded TF gene that regulates oxidative phosphorylation in human cells [40]. Together, these results suggest that increased ZNF682 occupancy in combination with reduced KLF and NFY promoter binding has an associated link to the liver metabolic shift from synthesis to break down of organic compounds as fish undergo parr-smolt transformation.

Following the parr-smolt transformation, the transition to a life in seawater is also known to be associated with additional changes in physiology in Atlantic salmon. Genes increasing in expression in seawater (Fig 2, cluster 1) were involved in ribosome biogenesis and their TFBS were associated with increased NFIX occupancy in seawater (Fig 7C), reported to impact ribosome biogenesis in mammals [31]. Another well known route to increased ribosome gene expression and protein synthesis is the induction of the mTOR pathway [72, 73]. Interestingly, seawater entry is known to trigger increased growth hormone levels in salmon [74, 75] and this hormone acts as a rapid activator of protein synthesis through the mTOR pathway [72]. Furthermore, seawater growth hormone increase can also be linked to the second group of TFs putatively involved in gene expression induction after seawater transition (Fig 2), namely JUN and FOS (Fig 7C). These genes, originally known as onco-genes, are also

19

409 responsive to growth hormones, and regulate cell proliferation and differentiation [32-34]. These TFs

410 provide the molecular basis for linking growth hormones to increased growth capacity of smolt in

411 seawater [4]. In our experiment freshwater control fish were larger than fish transferred to sea, but this

412 can be explained by a known initial suppression in growth and feeding followed by increased growth

413 rates [76]. Finally, genome-wide footprint signals (Fig 6) also pointed to large changes in the binding

414 of TFs involved in energy homeostasis after seawater entry [22-24], further underpinning the metabolic

415 gear shift. In conclusion, our data suggested that the genome regulatory dynamics in smolt livers across

416 the fresh- to seawater transition is likely driven to a large extent by an increase in circulating growth

417 hormone, resulting in activation of major regulatory pathways (e.g. JUN/FOS) for cell growth and

418 differentiation.

Materials and methods

Smoltification trial

421 Atlantic salmon eggs, provided by AquaGen Breeding Centre Kyrksæterøra, Norway, were sterilized at

422 the Norwegian University of Life Sciences (NMBU) fish lab and incubated at 350 to 372 day-degrees

423 until hatching. First feeding of fry was five weeks after hatching when the egg sac had been depleted.

424 Fry were reared in two replicate tanks and on a standard commercial diet high in EPA and DHA fats for

425 the duration of the trial. Fish occasionally needed to be euthanized as they grew to maintain adequate

426 dissolved oxygen levels in the tanks. Sampling began 21 weeks after first feeding as week 1, and again

427 at weeks 10, 19, and 25. Sampled fish were euthanized by a blow to the head and samples of liver tissue

428 were cut into ~5 mm cubes, placed in RNAlater, and incubated for at least 30 minutes at room

429 temperature before long-term storage at -20°C. One week after the first sampling, some fish from each

430 tank were transferred to replicate photoperiod control tanks where the day length remained unchanged.

431 At the same time, the experimental tanks' photoperiod was switched to "winter-like" lighting conditions

432 with 8 hours of light per day for 8 weeks to trigger smoltification before returning to "spring-like"

433 conditions with 24 hours of light per day. Immediately after the week 19 sampling, some fish from each

434 experimental tank were transferred to seawater conditions at the Norwegian Institute for Water Research

435   (NIVA), Solbergstranda, Norway. UV-sterilized seawater used in this life-stage had a salinity of 3%-

436   3.5% and was obtained from the Oslofjord. Fish were sedated before transport and allowed to

437   acclimatize for several hours before being slowly introduced to the new water conditions. The fish that

438   were not transferred to seawater were sampled as freshwater controls at the same time as the

439   experimental fish. All animals used in this study were handled in accordance with the Norwegian

440   Animal Welfare Act of 19th June 2009.

RNA sequencing

442   For RNA sequencing we extracted total RNA of liver samples from experimental and control groups

443   taken on weeks 1, 10, 19, and 25 in replicates of four with the RNeasy Plus Universal Kit (QIAGEN).

444   Concentration was determined with a nanodrop 8000 spectrophotometer (Thermo Scientific) and

445   quality was assessed by running on a 2100 bioanalyzer using the RNA 6000 Nano Kit (Agilent).

446   Extracted RNA with an RNA integrity number (RIN) of at least eight was used to make RNA-seq

447   libraries using the TruSeq Stranded mRNA HT Sample Prep Kit (Illumina). Mean length and library

448   concentration was determined by running libraries on a 2100 bioanalyzer using a DNA 1000 Kit

449   (Agilent). RNA-seq libraries were sequenced by the Norwegian Sequencing Center (Oslo, Norway) on

450   an Illumina HiSeq 4000 using 100 bp single end reads and at a depth of 25-43M reads per sample.

Gene expression quantification

452   Gene expression was quantified from RNA-seq fastq files through the nf-core rnaseq pipeline (v3.9),

453   which involves quality control, read trimming and filtering, read alignments to the Atlantic salmon

454   genome and gene annotations (NCBI refseq 100: GCF_000233375.1_ICSASG_v2) with STAR aligner,

455   and read quantification from alignment with the salmon program. See pipeline documentation for

456   further details on all steps: nf-co.re/rnaseq. Gene level counts, length scaled, were used for differential

457   expression testing, and gene transcript per million (TPM) values used for visualizations including

458   expression heatmaps and line plots. A PCA of gene TPMs showed one sample at week 10

459   (week_10_2_3, Biosample: SAMEA14383461) as an outlier (Fig S2) so we removed this sample from

460   the analysis.

Differential expression analysis

461 Differentially expressed genes (DEGs) were tested for first differences across all experimental group

463 time points using an ANOVA-like test with edgeR R package (v3.36) [77], using the generalized linear

464 model and quasi-likelihood F-test function (glmQLFTest), testing for differences between weeks 1, 10,

465 19, and 25. DEGs were chosen from the results using an FDR cutoff of <0.05. Euclidean distances of

466 DEG were calculated based on TPM values over the samples, and the DEGs separated into 7 clusters.

467 We chose 7 clusters based on observing patterns in the heatmap of expression and comparing the sum

468 of squares within and between different numbers of clusters. DEGs had to have correlation >0.5 to the

469 mean expression values of their assigned cluster, otherwise they were excluded from the cluster. DEGs

470 were also tested between experimental and control groups (short and long photoperiod history,

471 respectively) at week 10 and 19 separately, in pair-wise exact tests with edgeR (v3.36), choosing DEGs

472 with an FDR cutoff of <0.05. Enrichment of KEGG pathways in sets of DEGs was performed with the

473 clusterProfiler R package (v4.2.2), using the pathway data for Atlantic salmon genes within the KEGG

474 database.

ATAC sequencing

476 The protocol for the ATAC assay was based on that in Buenrostro et al. 2013 [78]. Two replicate liver

477 tissue samples were used from the previous sampling of the experimental group on weeks 1, 10, 19 and

478 25. The liver tissues were washed and perfused with cold PBS to remove blood before being dissociated

479 and strained through a cell strainer. The nuclei were isolated from cell homogenate by centrifugation

480 and counted on an automated cell counter (TC20 BioRad, range 4-6 um). Transposition of 100k (weeks

481 1, 19 and 25) and 75k (week 10) nuclei was performed by Tn5 transposase from Nextera DNA Library

482 Preparation kit. The resulting DNA fragments were purified and stored at -20°C. PCR Amplification

483 with addition of sequencing indexes (Nextera DNA CD) were done according to Buenrostro et al. 2015

484 [79], with a test PCR performed to determine the correct number of amplification cycles. The ATAC

485 libraries were cleaned by Ampure XP beads and assessed by BioAnalyser (Agilent) using High

486 sensitivity chips. Quantity of libraries were determined by using Qubit Fluorometer (Thermo). Mean

487   insert size for the libraries was 190 bp. Sequencing was done on a HiSeqX lane using 150 bp paired-

488   end reads and at a depth of 55-72M reads per sample.

ATAC peak calling

490   Calling of ATAC-seq peaks was done through the nf-core atacseq pipeline (v1.2.1), which involves

491   quality control, read trimming and filtering, read alignments to the Atlantic salmon genome (BWA

492   aligner), and calling of narrow peaks per sample as well as a unified narrow peak set across all samples

493   (MACS2 peak-caller). Data for QC results including PCA of samples, intersection of peaks sets, peak

494   distances to TSS, and peak genomic locations, were also computed through the pipeline. See pipeline

495   documentation for further details on all steps: nf-co.re/atacseq.

TF footprinting

497   TF footing in the unified ATAC peak set previously generated was done using the TOBIAS program

498   (v7.14.0) [80]. With it, we identified within peaks using the ATAC-seq read alignment BAM files for

499   each week (reads from replicates combined) 'footprints' (i.e. dips in read depth within peaks), indicative

500   of TF proteins binding to the DNA and locally blocking transposase activity during the ATAC protocol.

501   We used a set of TFBS motifs from the JASPER database (2020 CORE vertebrates non-redundant) to

502   associate these footprints with specific TFs. Peaks were associated to a gene by closest proximity to the

503   TSS during the atacseq pipeline. A blacklist file was used to mask simple repetitive regions in the

504   genome from analysis (generated in-house). Data for the genome-wide changes in TF binding was taken

505   from the 'bindetect_results.txt' file produced by TOBIAS, plotting the change in TF binding scores

506   between weeks against their p-values. The number of bound sites for each TF was scaled across weeks

507   and used for the heatmap visualization of differences. We identified TFs changing in response to salinity

508   or photoperiod by intersecting TF binding results between the different weeks. With a $\log_2$ fold change

509   cutoff of >0.1, TFs that had an increase in binding in week 25 compared to both weeks 1 and 19 were

510   assigned as 'sea', and inversely those with a decrease assigned as 'fresh'. Similarly for photoperiod

511   those increasing in week 10 compared to 1 and 19 were assigned 'short' and those decreasing were

512   assigned 'long'. We tested for the enrichment of certain TF binding patterns (which weeks TFBS were

513   bound) within the gene expression clusters previously identified. For this test we used the peak-gene

514   annotation data mentioned previously to assign the TFBS to genes. Then for each combination of TFBS

515   motif type, expression cluster, and TF binding pattern, we used a Fisher's exact test to test if motifs had

516   more often a specific TF binding pattern given a specific expression cluster, than compared to the total

517   background numbers (see Fig 7D for a diagram of the test). Results for binding patterns that did not

518   involve a change, i.e. bound at all weeks or no weeks, were not shown in the results.

Reduced Representation Bisulfite Sequencing

520   Livers from four fish per time point (three fish for week 25) were sampled and liver tissue was stored

521   on RNAlater at -20°C. The samples were processed with Ovation RRBS Methyl-Seq System (NuGen)

522   and bisulfite treatment was done with the Epitect Fast Bisulfite Conversion kit (Qiagen). RRBS libraries

523   were controlled with a BioAnalyser (Agilent) machine on DNA1000 chips. Paired-end sequencing was

524   performed by Novogene with a HiSeq X sequencing (Illumina). The mean library insert size was 168

525   bp and read depth was 26-40M reads.

Alignment of bisulfite-treated reads and cytosine methylation calls

527   Quality trimming of reads was done with Trim Galore (v0.6.4) [81] and adapters were removed with

528   cutadapt (v2.7) [82]. Bismark Bisulfite Mapper (v0.22.3) [81] was run with Bowtie 2 [83] against the

529   bisulfite genome of Atlantic salmon (ICSASG_v2) [84] with the specified parameters: -q --score-min

530   L,0,-0.2 --ignore-quals --no-mixed --no-discordant --dovetail --maxins 500. Alignment to

531   complementary strands were ignored by default. About 40-50% of the reads were mapped to the

532   genome. Methylated cytosines in a CpG context were extracted from the report.txt-files produced by

533   the Bismark methylation extractor. The resulting coverage files containing methylated and

534   unmethylated CpG loci for each sample was first filtered for known SNPs in the salmon genome then

535   used in the analysis of differential methylation. Coverage distribution around transcription start sites

536   (TSS) and 20 kb upstream and downstream showed that the highest coverage of reads was found nearby

537   TSS (Fig S3B) indicating that MSPI digestion of CCGGs have resulted in enrichment around TSS, as

538   expected by the RRBS method. Using genome annotation information, we classified CpGs according

539   to their genomic context (Fig S3C).

Differential methylation analysis

541   Samples were first organized with the R package methylKit (v1.9.4) [85] and the CpG loci were filtered

542   by read coverage, discarding those below 10 reads per locus or more than 99.9th percentile of coverage

543   in each sample, and those not to chromosomes. CpG loci between replicates were merged, keeping

544   those present in at least three of the samples. The differential methylation analysis was done with an

545   ANOVA-like analysis test of edgeR [77], contrasting the counts of methylated reads at different time

546   points. Differentially methylated CpGs (DMC) were called with an FDR <0.05. A heatmap of the

547   differentially methylated CpGs shows row scaled methylation percentage values of DMCs (Fig S3F).

Data availability

549   Sequencing data is in the European Nucleotide database for RNA-seq (PRJEB52829), ATAC-seq

550   (PRJEB65073), and RRBS (PRJEB60411). Code for running all steps of the analysis and generating

551   results and figures is available on gitlab (gitlab.com/sandve-lab/GSFsmolt).

Acknowledgments

References

556   1.   Hoar WS. 4 The Physiology of Smolting Salmonids. In: Hoar WS, Randall DJ, editors. Fish

557   Physiology. 11: Academic Press; 1988. p. 275-343.

558   2.   McCormick SD, Moriyama S, Björnsson BT. Low temperature limits photoperiod control of

559   smolting in Atlantic salmon through endocrine mechanisms. American Journal of Physiology-

Regulatory, Integrative and Comparative Physiology. 2000;278(5):R1352-R61. doi: 10.1152/ajpregu.2000.278.5.R1352. PubMed PMID: 10801307.

3.   Iversen M, Mulugeta T, Gellein Blikeng B, West AC, Jørgensen EH, Rød Sandven S, et al. RNA profiling identifies novel, photoperiod-history dependent markers associated with enhanced saltwater performance in juvenile Atlantic salmon. PLOS ONE. 2020;15(4):e0227496. doi: 10.1371/journal.pone.0227496.

4.   McCormick SD, Regish AM, Christensen AK. Distinct freshwater and seawater isoforms of Na+/K+-ATPase in gill chloride cells of Atlantic salmon. J Exp Biol. 2009;212(24):3994-4001. doi: 10.1242/jeb.037275.

5.   West AC, Mizoro Y, Wood SH, Ince LM, Iversen M, Jørgensen EH, et al. Immunologic Profiling of the Atlantic Salmon Gill by Single Nuclei Transcriptomics. Frontiers in Immunology. 2021;12. doi: 10.3389/fimmu.2021.669889.

6.   Sheridan MA. Alterations in lipid metabolism accompanying smoltification and seawater adaptation of salmonid fish. Aquaculture. 1989;82(1):191-203. doi: https://doi.org/10.1016/0044-8486(89)90408-0.

7.   Sheridan MA, Woo NYS, Bern HA. Changes in the rates of glycogenesis, glycogenolysis, lipogenesis, and lipolysis in selected tissues of the coho salmon (Oncorhynchus kisutch) associated with parr-smolt transformation. Journal of Experimental Zoology. 1985;236(1):35-44. doi: https://doi.org/10.1002/jez.1402360106.

8.   McCormick SD. 5 - Smolt Physiology and Endocrinology. In: McCormick SD, Farrell AP, Brauner CJ, editors. Fish Physiology. 32: Academic Press; 2012. p. 199-251.

9.   Solbakken VA, Hansen T, Stefansson SO. Effects of photoperiod and temperature on growth and parr-smolt transformation in Atlantic salmon (Salmo salar L.) and subsequent performance in seawater. Aquaculture. 1994;121(1):13-27. doi: https://doi.org/10.1016/0044-8486(94)90004-3.

10.   Strand JET, Hazlerigg D, Jørgensen EH. Photoperiod revisited: is there a critical day length for triggering a complete parr–smolt transformation in Atlantic salmon Salmo salar? J Fish Biol. 2018;93(3):440-8. doi: https://doi.org/10.1111/jfb.13760.

587   11.   Iversen M, Mulugeta T, West AC, Jørgensen EH, Martin SAM, Sandve SR, et al. Photoperiod-

588   dependent developmental reprogramming of the transcriptional response to seawater entry in Atlantic

589   salmon (Salmo salar). G3 Genes|Genomes|Genetics. 2021;11(4). doi: 10.1093/g3journal/jkab072.

590   12.   Bell JG, Tocher DR, Farndale BM, Cox DI, McKinney RW, Sargent JR. The effect of dietary

591   lipid on polyunsaturated fatty acid metabolism in Atlantic salmon (Salmo salar) undergoing parr-smolt

592   transformation. Lipids. 1997;32(5):515-25. doi: 10.1007/s11745-997-0066-4.

593   13.   Tocher DR, Bell JG, Dick JR, Henderson RJ, McGhee F, Michell D, et al. Polyunsaturated fatty

594   acid metabolism in Atlantic salmon (Salmo salar) undergoing parr-smolt transformation and the effects

595   of   dietary   linseed   and   rapeseed   oils.   Fish   Physiol   Biochem.   2000;23(1):59-73.   doi:

596   10.1023/A:1007807201093.

597   14.   Gillard G, Harvey TN, Gjuvsland A, Jin Y, Thomassen M, Lien S, et al. Life-stage-associated

598   remodelling of lipid metabolism regulation in Atlantic salmon. Mol Ecol. 2018;27(5):1200-13. doi:

599   10.1111/mec.14533.

600   15.   Li LO, Klett EL, Coleman RA. Acyl-CoA synthesis, lipid metabolism and lipotoxicity. Biochim

601   Biophys Acta. 2010;1801(3):246-51. doi: https://doi.org/10.1016/j.bbalip.2009.09.024.

602   16.   Yen C-LE, Stone SJ, Koliwad S, Harris C, Farese RV. Thematic Review Series: Glycerolipids.

603   DGAT   enzymes   and   triacylglycerol   biosynthesis.   J   Lipid   Res.   2008;49(11):2283-301.   doi:

604   https://doi.org/10.1194/jlr.R800018-JLR200.

605   17.   Sul HS, Smith S. CHAPTER 6 - Fatty acid synthesis in eukaryotes. In: Vance DE, Vance JE,

606   editors. Biochemistry of Lipids, Lipoproteins and Membranes (Fifth Edition). San Diego: Elsevier;

607   2008. p. 155-90.

608   18.   Grevengoed TJ, Klett EL, Coleman RA. Acyl-CoA Metabolism and Partitioning. Annu Rev

609   Nutr. 2014;34(1):1-30. doi: 10.1146/annurev-nutr-071813-105541. PubMed PMID: 24819326.

610   19.   Tillander V, Alexson SEH, Cohen DE. Deactivating Fatty Acids: Acyl-CoA Thioesterase-

611   Mediated Control of Lipid Metabolism. Trends in Endocrinology & Metabolism. 2017;28(7):473-84.

612   doi: https://doi.org/10.1016/j.tem.2017.03.001.

613   20.   Jones G, Strugnell SA, DeLuca HF. Current Understanding of the Molecular Actions of Vitamin

614   D. Physiol Rev. 1998;78(4):1193-231. doi: 10.1152/physrev.1998.78.4.1193. PubMed PMID: 9790574.

615   21.   Pierens SL, Fraser DR. The origin and metabolism of vitamin D in rainbow trout. The Journal

616   of steroid biochemistry and molecular biology. 2015;145:58-64. doi: 10.1016/j.jsbmb.2014.10.005.

617   PubMed PMID: 25305412.

618   22.   Meinsohn M-C, Smith OE, Bertolin K, Murphy BD. The Orphan Nuclear Receptors

619   Steroidogenic Factor-1 and Liver Receptor Homolog-1: Structure, Regulation, and Essential Roles in

620   Mammalian Reproduction. Physiol Rev. 2019;99(2):1249-79. doi: 10.1152/physrev.00019.2018.

621   PubMed PMID: 30810078.

622   23.   Olbrot M, Rud J, Moss LG, Sharma A. Identification of β-cell-specific insulin gene

623   transcription factor RIPE3b1 as mammalian MafA. Proceedings of the National Academy of Sciences.

624   2002;99(10):6737-42. doi: doi:10.1073/pnas.102168499.

625   24.   Yerra VG, Drosatos K. Specificity Proteins (SP) and Krüppel-like Factors (KLF) in Liver

626   Physiology and Pathology. International Journal of Molecular Sciences. 2023;24(5):4682. PubMed

627   PMID: doi:10.3390/ijms24054682.

628   25.   Kim YH, Lazar MA. Transcriptional Control of Circadian Rhythms and Metabolism: A Matter

629   of Time and Space. Endocr Rev. 2020;41(5):707-32. doi: 10.1210/endrev/bnaa014.

630   26.   Zhu B. Decoding the function and regulation of the mammalian 12-h clock. Journal of

631   Molecular Cell Biology. 2020;12(10):752-8. doi: 10.1093/jmcb/mjaa021.

632   27.   Lee C-H, Olson P, Hevener A, Mehl I, Chong L-W, Olefsky JM, et al. PPARδ regulates glucose

633   metabolism and insulin sensitivity. Proceedings of the National Academy of Sciences.

634   2006;103(9):3444-9. doi: doi:10.1073/pnas.0511253103.

635   28.   Carmona-Antoñanzas G, Tocher DR, Martinez-Rubio L, Leaver MJ. Conservation of lipid

636   metabolic gene transcriptional regulatory networks in fish and mammals. Gene. 2014;534(1):1-9. doi:

637   https://doi.org/10.1016/j.gene.2013.10.040.

638   29.   Huang K-W, Reebye V, Czysz K, Ciriello S, Dorman S, Reccia I, et al. Liver Activation of

639   Hepatocellular Nuclear Factor-4α by Small Activating RNA Rescues Dyslipidemia and Improves

640   Metabolic   Profile.   Molecular   Therapy   -   Nucleic   Acids.   2020;19:361-70.   doi:

641   https://doi.org/10.1016/j.omtn.2019.10.044.

642   30.   Mullur R Fau - Liu Y-Y, Liu Yy Fau - Brent GA, Brent GA. Thyroid hormone regulation of

643   metabolism. (1522-1210 (Electronic)).

644   31.   Walker M, Li Y, Morales-Hernandez A, Qi Q, Parupalli C, Brown SA, et al. An NFIX-mediated

645   regulatory network governs the balance of hematopoietic stem and progenitor cells during

646   hematopoiesis. Blood Advances. 2022. doi: 10.1182/bloodadvances.2022007811.

647   32.   Hernandez JM, Floyd DH, Weilbaecher KN, Green PL, Boris-Lawrie K. Multiple facets of junD

648   gene expression are atypical among AP-1 family members. Oncogene. 2008;27(35):4757-67. doi:

649   10.1038/onc.2008.120.

650   33.   Hess J, Angel P, Schorpp-Kistner M. AP-1 subunits: quarrel and harmony among siblings. J

651   Cell Sci. 2004;117(25):5965-73. doi: 10.1242/jcs.01589.

652   34.   Nisembaum LG, Martin P, Lecomte F, Falcón J. Melatonin and osmoregulation in fish: A focus

653   on Atlantic salmon Salmo salar smoltification. J Neuroendocrinol. 2021;33(3):e12955. doi:

654   https://doi.org/10.1111/jne.12955.

655   35.   Frey-Jakobs S, Hartberger JM, Fliegauf M, Bossen C, Wehmeyer ML, Neubauer JC, et al.

656   ZNF341 controls STAT3 expression and thereby immunocompetence. Science Immunology.

657   2018;3(24):eaat4941. doi: doi:10.1126/sciimmunol.aat4941.

658   36.   Golson ML, Kaestner KH. Fox transcription factors: from development to disease.

659   Development. 2016;143(24):4558-70. doi: 10.1242/dev.112672.

660   37.   Hannenhalli S, Kaestner KH. The evolution of Fox genes and their role in development and

661   disease. Nature Reviews Genetics. 2009;10(4):233-40. doi: 10.1038/nrg2523.

662   38.   Weiss RJ, Spahn PN, Toledo AG, Chiang AWT, Kellman BP, Li J, et al. ZNF263 is a

663   transcriptional regulator of heparin and heparan sulfate biosynthesis. Proceedings of the National

664   Academy of Sciences. 2020;117(17):9311-7. doi: doi:10.1073/pnas.1920880117.

665   39.   Yoon HS, Scharer CD, Majumder P, Davis CW, Butler R, Zinzow-Kramer W, et al. ZBTB32 Is

666   an Early Repressor of the CIITA and MHC Class II Gene Expression during B Cell Differentiation to

667   Plasma Cells. The Journal of Immunology. 2012;189(5):2393-403. doi: 10.4049/jimmunol.1103371.

668   40.   Arroyo JD, Jourdain AA, Calvo SE, Ballarano CA, Doench JG, Root DE, et al. A Genome-wide

669   CRISPR Death Screen Identifies Genes Essential for Oxidative Phosphorylation. Cell Metabolism.

670   2016;24(6):875-85. doi: https://doi.org/10.1016/j.cmet.2016.08.017.

671   41.   Su J, Morgani SM, David CJ, Wang Q, Er EE, Huang Y-H, et al. TGF-β orchestrates fibrogenic

672   and developmental EMTs via the RAS effector RREB1. Nature. 2020;577(7791):566-71. doi:

673   10.1038/s41586-019-1897-5.

674   42.   Thiagalingam A, Bustros Ad, Borges M, Jasti R, Compton D, Diamond L, et al. RREB-1, a

675   Novel Zinc Finger Protein, Is Involved in the Differentiation Response to Ras in Human Medullary

676   Thyroid Carcinomas. Mol Cell Biol. 1996;16(10):5335-45. doi: 10.1128/MCB.16.10.5335.

677   43.   Wung BS, Cheng JJ, Chao YJ, Hsieh HJ, Wang DL. Modulation of Ras/Raf/Extracellular

678   Signal–Regulated Kinase Pathway by Reactive Oxygen Species Is Involved in Cyclic Strain–Induced

679   Early Growth Response-1 Gene Expression in Endothelial Cells. Circul Res. 1999;84(7):804-12. doi:

680   doi:10.1161/01.RES.84.7.804.

681   44.   Reed BD, Charos AE, Szekely AM, Weissman SM, Snyder M. Genome-Wide Occupancy of

682   SREBP1 and Its Partners NFY and SP1 Reveals Novel Functional Roles and Combinatorial Regulation

683   of Distinct Classes of Genes. PLoS Genet. 2008;4(7):e1000133. doi: 10.1371/journal.pgen.1000133.

684   45.   Versteyhe S, Klaproth B, Borup R, Palsgaard J, Jensen M, Gray S, et al. IGF-I, IGF-II, and

685   Insulin Stimulate Different Gene Expression Responses through Binding to the IGF-I Receptor.

686   Frontiers in Endocrinology. 2013;4. doi: 10.3389/fendo.2013.00098.

687   46.   Ye D, Lou G, Zhang T, Dong F, Liu Y. MiR-17 family-mediated regulation of Pknox1 influences

688   hepatic   steatosis   and   insulin   signaling.   J   Cell   Mol   Med.   2018;22(12):6167-75.   doi:

689   https://doi.org/10.1111/jcmm.13902.

690   47.   Hunter AL, Pelekanou CE, Adamson A, Downton P, Barron NJ, Cornfield T, et al. Nuclear

691   receptor REVERBα is a state-dependent regulator of liver energy metabolism. Proceedings of the

692   National Academy of Sciences. 2020;117(41):25869-79. doi: doi:10.1073/pnas.2005330117.

693   48.   Oishi Y, Manabe I. Krüppel-Like Factors in Metabolic Homeostasis and Cardiometabolic

694   Disease. Frontiers in Cardiovascular Medicine. 2018;5. doi: 10.3389/fcvm.2018.00069.

695   49.   Pisam M, Prunet P, Boeuf G, Jrambourg A. Ultrastructural features of chloride cells in the gill

696   epithelium of the atlantic salmon, Salmo salar, and their modifications during smoltification. American

697   Journal of Anatomy. 1988;183(3):235-44. doi: https://doi.org/10.1002/aja.1001830306.

698   50.   Evans DH, Piermarini PM, Choe KP. The Multifunctional Fish Gill: Dominant Site of Gas

699   Exchange, Osmoregulation, Acid-Base Regulation, and Excretion of Nitrogenous Waste. Physiol Rev.

700   2005;85(1):97-177. doi: 10.1152/physrev.00050.2003. PubMed PMID: 15618479.

701   51.   Kiilerich P, Kristiansen K, Madsen SS. Cortisol regulation of ion transporter mRNA in Atlantic

702   salmon gill and the effect of salinity on the signaling pathway. J Endocrinol. 2007;194(2):417-27. doi:

703   10.1677/JOE-07-0185.

704   52.   Nilsen TO, Ebbesson LOE, Madsen SS, McCormick SD, Andersson E, Björnsson BrT, et al.

705   Differential expression of gill Na+,K+-ATPaseα- and β-subunits, Na+,K+,2Cl-cotransporter and CFTR

706   anion channel in juvenile anadromous and landlocked Atlantic salmon Salmo salar. J Exp Biol.

707   2007;210(16):2885-96. doi: 10.1242/jeb.002873.

708   53.   Tipsmark CK, Jørgensen C, Brande-Lavridsen N, Engelund M, Olesen JH, Madsen SS. Effects

709   of cortisol, growth hormone and prolactin on gill claudin expression in Atlantic salmon. Gen Comp

710   Endocrinol. 2009;163(3):270-7. doi: https://doi.org/10.1016/j.ygcen.2009.04.020.

711   54.   Itokazu Y, Käkelä R, Piironen J, Guan XL, Kiiskinen P, Vornanen M. Gill tissue lipids of salmon

712   (Salmo salar L.) presmolts and smolts from anadromous and landlocked populations. Comparative

713   Biochemistry and Physiology Part A: Molecular & Integrative Physiology. 2014;172:39-45. doi:

714   https://doi.org/10.1016/j.cbpa.2014.01.020.

715   55.   Ackman RG. Characteristics of the fatty acid composition and biochemistry of some fresh-

716   water fish oils and lipids in comparison with marine oils and lipids. Comparative Biochemistry and

717   Physiology. 1967;22(3):907-22. doi: https://doi.org/10.1016/0010-406X(67)90781-5.

718   56.   Sheridan MA, Allen WV, Kerstetter TH. Changes in the fatty acid composition of steelhead

719   trout, Salmo gairdnerii Richardson, associated with parr-smolt transformation. Comparative

720   Biochemistry and Physiology Part B: Comparative Biochemistry. 1985;80(4):671-6. doi:

721   https://doi.org/10.1016/0305-0491(85)90444-4.

57.   Björnsson BT, Thorarensen H, Hirano T, Ogasawara T, Kristinsson JB. Photoperiod and temperature affect plasma growth hormone levels, growth, condition factor and hypoosmoregulatory ability of juvenile Atlantic salmon (Salmo salar) during parr-smolt transformation. Aquaculture. 1989;82(1):77-91. doi: https://doi.org/10.1016/0044-8486(89)90397-9.

58.   Berge ÅI, Berg A, Barnung T, Hansen T, Fyhn HJ, Stefansson SO. Development of salinity tolerance in underyearling smolts of Atlantic salmon (Salmo salar) reared under different photoperiods. Can J Fish Aquat Sci. 1995;52(2):243-51. doi: 10.1139/f95-024.

59.   Duston J, Saunders RL. Advancing smolting to autumn in age 0+ Atlantic salmon by photoperiod, and long-term performance in sea water. Aquaculture. 1995;135(4):295-309. doi: https://doi.org/10.1016/0044-8486(95)01034-3.

60.   McCormick SD, Björnsson BT, Sheridan M, Eilerlson C, Carey JB, O'Dea M. Increased daylength stimulates plasma growth hormone and gill Na+, K+-ATPase in Atlantic salmon (Salmo salar). Journal of Comparative Physiology B. 1995;165(4):245-54. doi: 10.1007/BF00367308.

61.   McCormick SD, Shrimpton JM, Moriyama S, Björnsson BT. Differential hormonal responses of Atlantic salmon parr and smolt to increased daylength: A possible developmental basis for smolting. Aquaculture. 2007;273(2):337-44. doi: https://doi.org/10.1016/j.aquaculture.2007.10.015.

62.   Duncan NJ, Bromage N. The effect of different periods of constant short days on smoltification in juvenile Atlantic salmon (Salmo salar). Aquaculture. 1998;168(1):369-86. doi: https://doi.org/10.1016/S0044-8486(98)00363-9.

63.   Handeland SO, Stefansson SO. Photoperiod control and influence of body size on off-season parr–smolt transformation and post-smolt growth. Aquaculture. 2001;192(2):291-307. doi: https://doi.org/10.1016/S0044-8486(00)00457-9.

64.   Stefansson SO, Nilsen TO, Ebbesson LOE, Wargelius A, Madsen SS, Björnsson BT, et al. Molecular mechanisms of continuous light inhibition of Atlantic salmon parr–smolt transformation. Aquaculture. 2007;273(2):235-45. doi: https://doi.org/10.1016/j.aquaculture.2007.10.005.

65.   Ross AW, Webster CA, Mercer JG, Moar KM, Ebling FJ, Schuhler S, et al. Photoperiodic Regulation of Hypothalamic Retinoid Signaling: Association of Retinoid X Receptor γ with Body Weight. Endocrinology. 2004;145(1):13-20. doi: 10.1210/en.2003-0838.

750 66. Verma R, Haldar C. Photoperiodic modulation of thyroid hormone receptor (TR-α), deiodinase-

751 2 (Dio-2) and glucose transporters (GLUT 1 and GLUT 4) expression in testis of adult golden hamster,

752 Mesocricetus auratus. J Photochem Photobiol B: Biol. 2016;165:351-8. doi:

753 https://doi.org/10.1016/j.jphotobiol.2016.10.036.

754 67. Morán P, Pérez-Figueroa A. Methylation changes associated with early maturation stages in the

755 Atlantic salmon. BMC Genet. 2011;12(1):86. doi: 10.1186/1471-2156-12-86.

756 68. Mohamed AR, Naval-Sanchez M, Menzies M, Evans B, King H, Reverter A, et al. Leveraging

757 transcriptome and epigenome landscapes to infer regulatory networks during the onset of sexual

758 maturation. BMC Genomics. 2022;23(1):413. doi: 10.1186/s12864-022-08514-8.

759 69. Riviere G, He Y, Tecchio S, Crowell E, Gras M, Sourdaine P, et al. Dynamics of DNA

760 methylomes underlie oyster development. PLoS Genet. 2017;13(6):e1006807. doi:

761 10.1371/journal.pgen.1006807.

762 70. Gegner J, Vogel H, Billion A, Förster F, Vilcinskas A. Complete Metamorphosis in Manduca

763 sexta Involves Specific Changes in DNA Methylation Patterns. Frontiers in Ecology and Evolution.

764 2021;9. doi: 10.3389/fevo.2021.646281.

765 71. Cardoso-Júnior CAM, Yagound B, Ronai I, Remnant EJ, Hartfelder K, Oldroyd BP. DNA

766 methylation is not a driver of gene expression reprogramming in young honey bee workers. Mol Ecol.

767 2021;30(19):4804-18. doi: https://doi.org/10.1111/mec.16098.

768 72. Hayashi AA, Proud CG. The rapid activation of protein synthesis by growth hormone requires

769 signaling through mTOR. American Journal of Physiology-Endocrinology and Metabolism.

770 2007;292(6):E1647-E55. doi: 10.1152/ajpendo.00674.2006. PubMed PMID: 17284572.

771 73. Laplante M, Sabatini DM. Regulation of mTORC1 and its impact on gene expression at a

772 glance. (1477-9137 (Electronic)).

773 74. Handeland SO, Björnsson, Arnesen AM, Stefansson SO. Seawater adaptation and growth of

774 post-smolt Atlantic salmon (Salmo salar) of wild and farmed strains. Aquaculture. 2003;220(1):367-84.

775 doi: https://doi.org/10.1016/S0044-8486(02)00508-2.

776   75.   Sakamoto T, McCormick SD, Hirano T. Osmoregulatory actions of growth hormone and its

777   mode of action in salmonids: A review. Fish Physiol Biochem. 1993;11(1):155-64. doi:

778   10.1007/BF00004562.

779   76.   Usher ML, Talbot C, Eddy FB. Effects of transfer to seawater on growth and feeding in Atlantic

780   salmon smolts (Salmo salar L.). Aquaculture. 1991;94(4):309-26. doi: https://doi.org/10.1016/0044-

781   8486(91)90176-8.

782   77.   Robinson MD, McCarthy DJ, Smyth GK. edgeR: a Bioconductor package for differential

783   expression analysis of digital gene expression data. Bioinformatics. 2009;26(1):139-40. doi:

784   10.1093/bioinformatics/btp616.

785   78.   Buenrostro JD, Giresi PG, Zaba LC, Chang HY, Greenleaf WJ. Transposition of native

786   chromatin for fast and sensitive epigenomic profiling of open chromatin, DNA-binding proteins and

787   nucleosome position. Nat Methods. 2013;10(12):1213-8. doi: 10.1038/nmeth.2688.

788   79.   Buenrostro JD, Wu B, Chang HY, Greenleaf WJ. ATAC-seq: A Method for Assaying Chromatin

789   Accessibility Genome-Wide. Current Protocols in Molecular Biology. 2015;109(1):21.9.1-.9.9. doi:

790   https://doi.org/10.1002/0471142727.mb2129s109.

791   80.   Bentsen M, Goymann P, Schultheis H, Klee K, Petrova A, Wiegandt R, et al. ATAC-seq

792   footprinting unravels kinetics of transcription factor binding during zygotic genome activation. Nature

793   Communications. 2020;11(1):4267. doi: 10.1038/s41467-020-18035-1.

794   81.   Krueger F, Andrews SR. Bismark: a flexible aligner and methylation caller for Bisulfite-Seq

795   applications. Bioinformatics. 2011;27(11):1571-2. doi: 10.1093/bioinformatics/btr167.

796   82.   Martin M. Cutadapt removes adapter sequences from high-throughput sequencing reads.

797   EMBnetjournal; Vol 17, No 1: Next Generation Sequencing Data AnalysisDO - 1014806/ej171200.

798   2011.

799   83.   Langmead B, Salzberg SL. Fast gapped-read alignment with Bowtie 2. Nat Methods.

800   2012;9(4):357-9. doi: 10.1038/nmeth.1923.

801   84.   Lien S, Koop BF, Sandve SR, Miller JR, Kent MP, Nome T, et al. The Atlantic salmon genome

802   provides insights into rediploidization. Nature. 2016;533(7602):200-5. doi: 10.1038/nature17164.

803   85.   Akalin A, Kormaksson M, Li S, Garrett-Bakelman FE, Figueroa ME, Melnick A, et al.

804   methylKit: a comprehensive R package for the analysis of genome-wide DNA methylation profiles.

805   Genome Biology. 2012;13(10):R87. doi: 10.1186/gb-2012-13-10-r87.

806

Supplementary material

807

808   **Fig S1. Gene expression changes in response to salinity.**

809   Relative liver expression of genes differentially expressed (FDR <0.05) between the seawater exposed

810   experimental group and freshwater control group at week 25. Genes are marked to the right if

811   differentially expressed at week 25, green if higher in seawater, blue if higher in freshwater.

812   **Fig S2. Principal component analysis of gene expression differences between samples.**

813   A) Similarity between all samples in the study, by principal components (PC) of gene expression.

814   Experimental samples are colored red, and control samples for the same time points are colored gray.

815   Labeled are potential outlier samples. B) Effect of removing sample 'week_10_2_3' from the PCA.

816   **Fig S3. Methylated CpGs from RRBS assay.**

817   A) Similarity of samples by principal components (PC) of the read coverage of consensus CpGs. B)

818   Genomic context of the differentially methylated CpGs. C) Heatmap of methylation values of

819   differentially methylated CpGs during the smoltification trial. D) Density of correlation values between

820   differentially methylated CpGs and gene expression levels, and density of correlation levels between

821   random gene-CpG pairs.

822   **Table S1. Phenotypic data of sampled Atlantic salmon.**

823   Phenotype data of Atlantic salmon used in this study. Columns provide: Unique fish identifier (*Fish*

824   *ID*), week fish was sampled (*Week #*), tank number (*Tank #*), fish number (*Fish #*), date fish was sampled

825   (*Date sampled*), fish weight (*Weight (g)*), fish length (*Length (mm)*), fish sex (*sex (M/F)*).

826 **Table S2. Differentially expressed genes across smoltification.**

827 Atlantic salmon genes differentially expressed (FDR <0.05) between any time points across the

828 smoltification experiment. Columns provide: the NCBI id for genes (*gene_id*), available gene name

829 (*gene_name)*, description of coded protein (*description*), and expression cluster number genes were

830 assigned to (*deg_cluster*).

831 **Table S3. Differentially expressed genes in response to photoperiod at week 10.**

832 Atlantic salmon genes differentially expressed (FDR <0.05) between week 10 experimental samples

833 exposed prior to short photoperiod conditions, and week 10 control samples kept under continuous long

834 photoperiod conditions. Columns provide: the NCBI id for genes (*gene_id)*, available gene name

835 (*gene_name)*, description of coded protein (*description*), $\log_2$ fold change in expression of experiment

836 versus control values (*logFC)*, average expression across samples in $\log_2$ counts per million (logCPM),

837 p-value of the differential expression test (*PValue)*, false discovery rate adjusted p-value (*FDR*), and the

838 time point that was tested, in this case week 10 (*week*).

839 **Table S4. Differentially expressed genes in response to photoperiod at week 19.**

840 Atlantic salmon genes differentially expressed (FDR <0.05) between week 19 experimental samples

841 exposed prior to short photoperiod conditions, and week 19 control samples kept under continuous long

842 photoperiod conditions. Columns provide: the NCBI id for genes (*gene_id)*, available gene name

843 (*gene_name)*, description of coded protein (*description*), $\log_2$ fold change in expression of experiment

844 versus control values (*logFC)*, average expression across samples in $\log_2$ counts per million (logCPM),

845 p-value of the differential expression test (*PValue)*, false discovery rate adjusted p-value (*FDR*), and the

846 time point that was tested, in this case week 19 (*week*).

847 **Table S5. Differentially expressed genes in response to seawater transition.**

848 Atlantic salmon genes differentially expressed (FDR <0.05) between week 25 experimental samples

849 after transition to seawater conditions, and week 25 control samples kept under freshwater conditions.

850 Columns provide: the NCBI ID for genes (*gene_id)*, available gene name (*gene_name)*, description of

851   coded protein (*description*), log$_2$ fold change in expression of experiment versus control values (*logFC*),

852   average expression across samples in log$_2$ counts per million (*logCPM*), p-value of the differential

853   expression test (*PValue*), false discovery rate adjusted p-value (*FDR*).

854   **Table S6. Global changes in transcription factor binding.**

855   Results from TOBIAS ATAC-seq footprinting of transcription factor binding sites (TFBS) in the

856   Atlantic salmon genome, showing the global changes in transcription factor (TF) binding for all TF

857   motifs tested, across the different time points of the experiment. Columns provide: output file prefix of

858   TF name with motif ID (*output_prefix*), TF name (*name*), motif ID (*motif_id*), name of the TF's cluster

859   group (*cluster*), total number of TFBS (*total_tfbs*), columns for the mean score of TF binding across all

860   TFBS for each time point (columns *week_1_mean_score* to *week_25_mean_score*), total number of

861   bound TFBS for each time point (columns *week_10_bound* to *week_25_bound*), and the fold change

862   followed by the p-value of the significance of the change for each pair of different time points (columns

863   *week_1_week_10_change,*   *week_1_week_10_pvalue*   to   *week_19_week_25_change,*

864   *week_19_week_25_pvalue*).

865   **Table S7. Changes in transcription factor binding to salinity and photoperiod.**

866   Transcription factors (TF) with significe changes in global binding of transcription factor binding sites

867   (TFBS) between time points representing a concerted change due to experimental conditions. To

868   photoperiod conditions; week 1 (light) vs week 10 (dark), and week 10 (dark) vs 19 (light), or to salinity

869   conditions; week 1 (fresh) vs week 25 (sea), and week 19 (fresh) vs week 25 (sea). Columns provide:

870   TF name (*name*), time point comparison (*comparison*), p-value of the significance of the change

871   between time points (*pvalue*), the fold change in different of TF binding scores (*change*), the conditions

872   compared; photoperiod or salinity (*category*), the time point where positive change means more binding

873   (*week_A*), the time point where negative change means more binding (*week_B*), and the conditions

874   where there is significantly more binding of the TF (*sig*).

875   **Table S8. Enrichment in binding patterns of transcription factor binding sites of genes in**

876   **expression clusters.**

877   Results of Fisher's exact tests for the enrichment in different binding patterns of transcription factor

878   binding sites (TFBS) of genes in different expression clusters. Tested for each transcription factor (TF).

879   Columns provide: the gene expression cluster (*deg_cluster*), the binding pattern tested made up of 4

880   digits representing the 4 time points in chronological order with *0* equating to the TFBS not bound while

881   *1* is bound (*binding*), the total number of TFBS with the binding pattern associated by nearest proximity

882   to genes within the expression cluster (*count*), p-value of Fisher's exact test (*pval*), odds ratio of test

883   (*OR*), name of the TF motif for the TFBS (*TFBS_name*).

884   **Table S9. Differentially methylated CpGs**

885   CpG sites significantly differentially methylated between time points of the experiment (FDR <0.05).

886   Columns provide: Percentage score of the number of reads methylated at the CpG site for each time

887   point (columns *week_1_score* to *week_25_score*), unique position of site in Atlantic salmon genome

888   (*uniq_pos*), chromosome of site (*chr*), base position on chromosome (*locus*), $\log_2$ fold change in

889   methylated read count across time points (columns *week_10_week_1_logFC* to

890   *week_25_week_19_logFC*), average count of methylated reads across samples in $\log_2$ counts per million

891   (log*CPM*), p-value for significance in change between any time points (*PValue*), false discovery rate

892   adjusted p-value (*FDR*), associated gene's NCBI ID (*gene_id*), position of gene transcription start site

893   (TSS) (*tss*), gene strand position (*strand*), distance of gene TSS to CpG site (*distance*), start and end

894   positions of gene (*gene_start, gene_end*), gene width (*gene_width*), and type of genomic feature the

895   CpG site is located in (*genomic_feature*).